Three-Dimensional Structure of Conotoxin tx3a: An m-1 Branch Peptide of the M-Superfamily[†]

Owen M. McDougal,*[,‡] Matthew W. Turner,[‡] Andrew J. Ormond,[‡] and C. Dale Poulter[§]

Department of Chemistry and Biochemistry, Boise State University, Boise, Idaho 83725, and Department of Chemistry, University of Utah, Salt Lake City, Utah 84112

Received December 6, 2007; Revised Manuscript Received December 21, 2007

ABSTRACT: The M-superfamily, one of eight major conotoxin superfamilies found in the venom of the cone snail, contains a Cys framework with disulfide-linked loops labeled 1, 2, and 3 (-CC^{1}C^{2}C^{3}CC-). M-Superfamily conotoxins can be divided into the m-1, -2, -3, and -4 branches, based upon the number of residues located in the third Cys loop between the fourth and fifth Cys residues. Here we provide a three-dimensional solution structure for the m-1 conotoxin tx3a found in the venom of *Conus textile*. The 15-amino acid peptide, CCSWDVCDHPSCTCC, has disulfide bonds between Cys^1 and Cys^{14}, Cys^2 and Cys^{12}, and Cys^7 and Cys^{15} typical of the C1−C5, C2−C4, and C3−C6 connectivity pattern seen in m-1 branch peptides. The tertiary structure of tx3a was determined by two-dimensional ^{1}H NMR in combination with the combined assignment and dynamics algorithm for nuclear magnetic resonance (NMR) applications CYANA program. Input for structure calculations consisted of 62 inter- and intraproton, five φ angle, and four hydrogen bond constraints. The root-mean-square deviation values for the 20 final structures are 0.32 ± 0.07 and 0.84 ± 0.11 Å for the backbone and heavy atoms, respectively. Surprisingly, the structure of tx3a has a "triple-turn" motif seen in the m-2 branch conotoxin mr3a, which is absent in mr3e, the only other member of the m-1 branch of the M-superfamily whose structure is known. Interestingly, injection of tx3a into mice elicits an excitatory response similar to that of the m-2 branch peptide mr3a, even though the conotoxins have different disulfide connectivity patterns.

Cone snails are a class of predatory marine snail, which inject a potent nerve toxin into their prey by way of a disposable hollow tooth. All of the approximately 500 members of the genus *Conus* are venomous hunters of fish, worms, or snails (*1*). Cone snail venom is typically composed of 40−200 small peptides which range in size from 10 to 40 amino acids (*2*). The great diversity and specificity of *Conus* toxins, termed conotoxins, have been attributed to intense evolutionary pressures. The venom serves as a defense against predators and, in some cases, allows the slow moving snail to hunt rapidly moving prey (*3*).

It is the diversity, specificity, and simplicity of conotoxins that contribute to their usefulness as receptor probes. Conotoxins can inhibit or induce muscle contraction in mice, block sodium, potassium, or calcium channels, influence glutamate receptor binding, or cause behavioral changes in mice or other animals (*4*). The specificity shown by individual conotoxins provides the potential to isolate individual receptor types as well as to determine the essential elements for receptor−ligand binding (*5*).

Three-dimensional solution structures of conotoxins determined by NMR[1] spectroscopy have served as models for structure−function relationships. To date, structures for approximately 107 *Conus* peptides have been determined (*6*). The most studied of these peptides, the α-conotoxins, selectively bind to specific subunits of the nicotinic acetylcholine receptor (nAChR) (*7–13*). These studies have contributed to an understanding of how nAChRs function and to the development of compounds that specifically target individual receptor types. The α-conotoxins also demonstrate the potential of conotoxins in general to serve as potent and selective probes of closely related receptor types within the human body (*14*).

Conotoxins of a particular family generally have the same arrangement of cysteine residues in their primary sequence and the same cystine pattern and cause similar physiological effects in test animals, indicating that they target common receptor types. In contrast, the M-superfamily, which is characterized by the three-loop CC-C-C-CC cysteine arrangement, exhibits at least three distinct cystine patterns and a diversity of physiological effects in test animals. The superfamily consists of four branches, m-1, m-2, m-3, and m-4, defined by the number of residues between C4 and C5

[†] This work supported by NIH Grants GM 21328, GM 48677, and P20 RR016454 and MSTMRI Grant 6PR3381000154.

* To whom correspondence should be addressed: Department of Chemistry and Biochemistry, Boise State University, 1910 University Dr., MS 1520, Boise, ID 83725. Phone: (208) 426-3964. Fax: (208) 426-3027. E-mail: owenmcdougal@boisestate.edu.

[‡] Boise State University.

[§] University of Utah.

[1] Abbreviations: tx3a, member of the m-1 branch of the M-superfamily of conotoxins from *Conus textile*; mr3a, member of the m-2 branch of the M-superfamily of conotoxins from *Conus marmoreus*; mr3e, member of the m-1 branch of the M-superfamily of conotoxins from *C. marmoreus*; 1D, one-dimensional; 2D, two-dimensional; NMR, nuclear magnetic resonance; DQF-COSY, double-quantum-filtered 2D correlation spectroscopy; TOCSY, 2D total correlation spectroscopy; NOE, nuclear Overhauser effect; NOESY, 2D NOE spectroscopy; HPLC, high-pressure liquid chromatography; TFA, trifluoroacetic acid; ivc, intracerebral ventricular injection; ip, interperitoneal injection.

10.1021/bi702388b CCC: $40.75
Published on Web 01/19/2008

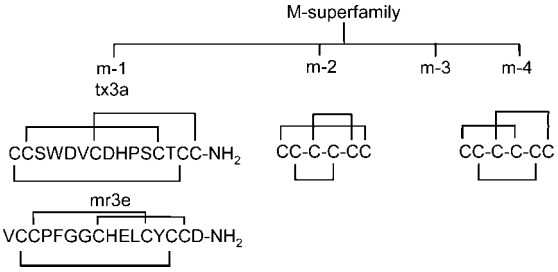

FIGURE 1: Summary of the four branches of the M-superfamily containing the conserved CC-CC-CC cysteine pattern with divergent cystine connectivity.

(i.e., loop 3) (*15*). The diversity of peptides exemplified in this superfamily is thought to enhance the cone snail's ability to survive. For example, the m-4 branch μ-, ψ-, and κM-conotoxins with the same disulfide connectivity have a diverse set of molecular targets (Na^+ channel, nicotinic acetylcholine receptor, and K^+ channel, respectively) (*15*).

There is considerable structural diversity among the M-superfamily conotoxins. Members of the m-1, m-2, and m-3 branches are smaller (12–19 amino acids) and contain disulfide connectivities different from those observed for the m-4 branch peptides (22–24 amino acids). The m-1 branch peptides mr3e and tx3a have C1−C5, C2−C4, and C3−C6 connectivity patterns (*16*). Other disulfide connectivities within the M-superfamily are C1−C6, C2−C4, C3−C5 for the m-2 branch and C1−C4, C2−C5, C3−C6 for the m-4 branch (Figure 1). While the receptors targeted by the m-4 branch peptides are well-established, those for the m-1, m-2, and m-3 branch peptides have not been determined. Members of the M-superfamily peptides appear to be very abundant in cone snail venom and presumably are important for survival of the mollusks. The lack of physiological data for m-1, m-2, and m-3 branch peptides has apparently discouraged the widespread pursuit of their three-dimensional structures. Currently, structures are available for only the m-1 branch peptide mr3e and the m-2 branch peptide mr3a. No representative structures have been reported for an m-3 branch peptide (*17, 18*). In contrast, there are several representative structures in the literature for the m-4 branch peptides, whose receptor targets have been determined (*19–22*).

Interest in tx3a, an m-1 branch conotoxin, arose because members of the M-superfamily appear to be present in every *Conus* species tested to date and the m-1, m-2, and m-3 conotoxins belong to a structurally and pharmacologically distinct group within the M-superfamily that has not been well-characterized. Physiologically, tx3a and mr3a have similar effects in mice and no apparent activity in fish (*15*). The observed activity is based on varying amounts of toxin administered to mice via intracerebral ventricular injection (ivc) or to fish via interperitoneal injection (ip). A screen for activity generally consists of injecting five mice and five fish with 2−10 nmol of toxin in 2 nmol increments and visually observing the behavioral effect of the toxin on the mice or fish. The ivc injection of conotoxin tx3a into 15-day-old mice caused hyperactivity at low doses (~2 nmol), which wore off after only a few minutes, and violent seizures followed by death at high doses (~10 nmol). The ip injection of tx3a in mice or fish did not result in an appreciable response. These physiological effects are analogous to those reported for the m-2 conotoxin mr3a (*15*). Corpuz et al. reported that the dose response, upon ivc injection of mr3a into 10-day-old mice, caused scratching at a low dose (<0.1 nmol/g), circular motion and barrel rolling at medium doses, and convulsion and death at a dose of 0.85 nmol/g. Intraperitoneally, injection into mice resulted in no observed response, nor did injection of mr3a into goldfish elicit a response at levels up to 2.5 nmol/g of body weight. Although the receptors are not known for either tx3a or mr3a, the observation that they elicit such dramatic effects in mice at nanomolar quantities yet do not affect fish indicates that these peptides may possess desirable receptor selectivity. To date, no biological actions have been reported for conotoxin mr3e. We now report the solution structure of conotoxin tx3a, which represents the second example of an m-1 branch peptide of the M-superfamily to be characterized by 2D ^{1}H NMR.

MATERIALS AND METHODS

Preparation of tx3a. NMR samples were prepared at a concentration of approximately 4.2 mM in either 100% D_2O (Cambridge Isotope Laboratories, Inc., Andover, MA) or a 9:1 (v/v) H_2O/D_2O mixture with 0.01% TFA (pH 4.0). Three successive lyophilizations in D_2O were performed to ensure complete exchange of labile protons. Two-dimensional ^{1}H NMR experiments and interpretation of spectra were based on established methods (*23, 24*).

NMR Spectroscopy. All NMR data were acquired at 11.75 T on a Varian INOVA 500 MHz NMR spectrometer at 4.0 °C. Proton DQF-COSY (*25*), NOESY (*26*), and TOCSY (*27*) spectra in D_2O were acquired with the transmitter set to 4.76 ppm and a spectral window of 4500 Hz, giving rise to FIDs of 4096 complex points in the ω_2 dimension. Spectra in H_2O were acquired with the transmitter set at 4.8 ppm and a spectral window of 6500 Hz, giving rise to FIDs of 4096 complex points in the ω_2 dimension. Transmitter presaturation was applied at the solvent frequency to suppress the H_2O resonance. Series of NOESY spectra were acquired with mixing times of 50, 100, and 200 ms. A TOCSY spectrum was acquired with a mixing time of 200 ms. Spectra were processed on a Silicon Graphics Indigo 2 and/or a Sun Spark 5 workstation using Varian VNMR software.

Restraint Set Generation. The $^3J_{NH\text{-}\alpha}$ values for Cys^2, Asp^5, Val^6, Cys^7, and Cys^{12} were extracted from a high-resolution 1D ^{1}H spectrum. Backbone dihedral φ angle restraints were set to $-120 \pm 40°$ for $^3J_{NH\text{-}\alpha}$ values greater than 7.5 Hz and to $-65 \pm 25°$ for a $^3J_{NH\text{-}\alpha}$ of less than 5 Hz. Inter- and intraproton distance ranges were derived from NOESY spectra recorded at 4 °C and mixing times of 50, 100, and 200 ms. A plot of cross-peak intensity versus mixing time allowed the initial slope of the NOE buildup to be calibrated. As a distance reference, the slope of the buildup for geminal protons was set to 1.8 Å. Restraints were set to 1.8–2.7, 1.8–3.3, and 1.8–5.0 Å for high, medium, and low slopes of NOE intensity, respectively, plotted against increasing mixing time. Only cross-peaks that demonstrated accurate depictions of the initial buildup over the times recorded were used for restraints (*28*).

Structure Calculations. One thousand initial structures generated from random starting conformations were input into the CYANA (version 2.1) software (*29*). The distance geometry and gradient minimization calculations were

Table 1: Proton Resonance Assignments for Conotoxin tx3a at 4 °C

residue	HN	α	β	other
Cys[1]	8.09	4.19	2.62, 2.26	
Cys[2]	8.04	4.14	3.34, 3.20	
Ser[3]	8.70	4.07	3.66, 3.66	
Trp[4]	8.45	3.94	3.09, 2.97	2H 7.10, 4H 7.41, 5H 6.65, 6H 7.00, 7H 7.20, NH 9.86
Asp[5]	7.98	4.56	2.75, 2.65	
Val[6]	7.45	4.30	1.84	γ 0.55, 0.52
Cys[7]	7.26	4.17	2.89, 2.08	
Asp[8]	8.61	4.10	3.68, 3.68	
His[9]	8.37	4.02	3.08, 3.00	2H 7.03, 4H 7.12
Pro[10]		4.13	2.05, 1.95	γ 1.74, 1.45; δ 3.33, 3.21
Ser[11]	7.38	4.26	2.86, 2.51	
Cys[12]	7.15	4.50	2.59, 2.32	
Thr[13]	8.90	4.04	3.99	γ 1.06
Cys[14]	8.82	4.90	2.95, 2.75	
Cys[15]	8.88	4.94	2.14, 2.01	

performed to find the conformations which best modeled the 62 upper and 17 lower distance limits, the five φ angles, the four hydrogen bonds, and the three disulfide bonds consistent with the NMR data and the molecular backbone, respectively. A pseudoatom correction of 0.5 Å was added to the upper bounds of restraints for methyl and methylene groups. The final set of 20 structures demonstrated an overall root-mean-square deviation among backbone atoms of 0.32 ± 0.07 Å.

RESULTS

Assignment of Resonances. The complete ^{1}H resonance assignment for tx3a was achieved using the method of Wüthrich (*23*) (see Table 1). A combination of DQF-COSY, NOESY, and TOCSY spectra acquired at 4 °C in both a 9:1 (v/v) H_2O/D_2O mixture and 100% D_2O were used to eliminate any ambiguities in assignment. Fourteen of the 15 amino acid spin systems for tx3a were identified in the

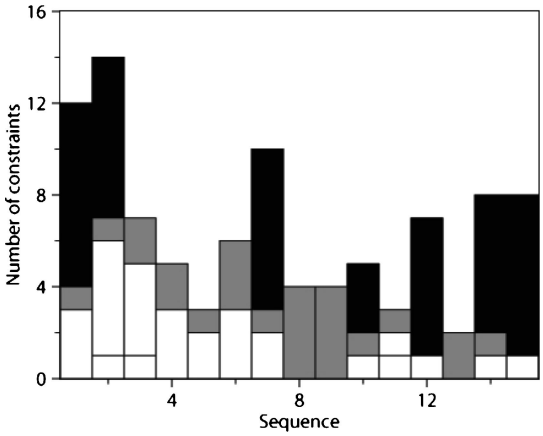

FIGURE 2: Distribution of distance constraints as a function of their residue number used for the structure determination of conotoxin tx3a. The white areas represent intraresidual constraints, light gray areas sequential constraints, dark gray areas medium-range NOEs ($d_{ij} \leq 5$ Å), and black areas long-range NOEs ($d_{ij} \geq 5$ Å).

Table 2: Restraints Used To Determine the Structure of tx3a

distance restraints	no.	dihedral restraints	no.
intraresidue	4	φ angle	5
sequential	26	hydrogen bond	4
medium	22	total	9
long	48		
total	100		

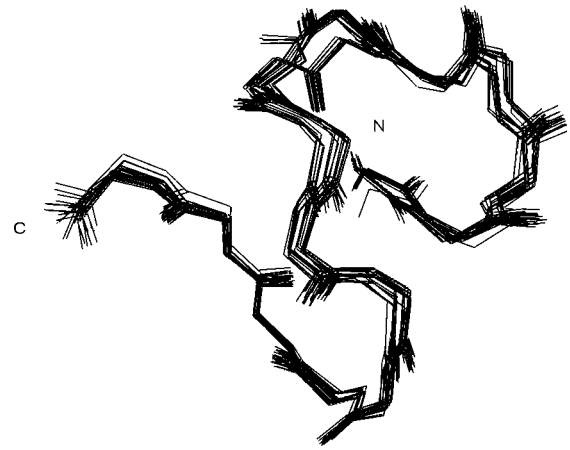

FIGURE 3: Overlay of the backbone atoms of tx3a for the final 20 structures generated by CYANA.

"fingerprint" region of a 200 ms mixing time TOCSY spectrum. The remaining residue, Pro[10], lacks a resonance in this region of the spectrum and was identified later. Ten of the spin systems were confirmed in the fingerprint region of a DQF-COSY spectrum and assigned to Cys[1], Cys[2], Ser[3], Asp[5], Val[6], Cys[7], Asp[8], Ser[11], Cys[12], and Thr[13]. Verification of α- and β-proton resonances and the location of the Pro[10] spin system were extracted from TOCSY and DQF-COSY spectra acquired in D_2O. A complete and thorough mapping of all amino acid spin systems was accomplished in this manner.

The assignment of spin systems to amino acids in the primary sequence of the peptide went as follows. The methyl region between 0.52 and 1.06 ppm in the TOCSY spectrum acquired in 90% H_2O provided information needed to identify Val[6] and Thr[13]. The two methyl resonances for Val[6] at 0.55 and 0.52 ppm were easily distinguished from the single methyl in Thr[13] at 1.06 ppm. Diagnostic resonances were also seen for His[9], Trp[4], and Pro[10]. The ring protons of His[9] and Trp[4] were found in the TOCSY spectrum acquired in D_2O between 6.65 and 9.86 ppm. Trp[4] was distinguished from His[9] by the proton on the nitrogen of the Trp[4] indole ring. This indole proton, which resonated at 9.86 ppm, is unique to tryptophan. The spin system assigned to Pro[10] originated at 4.13 ppm in the TOCSY spectrum acquired in D_2O. The δ-protons at 3.33 and 3.21 ppm were helpful for assigning resonances for Pro[10] because its α-proton at 4.13 ppm was within 0.04 ppm of the α-protons of Cys[2], Ser[3], Cys[7], and Asp[8]. A complete trace of the Pro[10] spin system was the only way to distinguish the amino acid from those with overlapping spin systems. The remaining amino acids, Cys[1], Cys[2], Ser[3], Asp[5], Cys[7], Asp[8], Ser[11], Cys[12], Cys[14], and Cys[15], all share the same AMX pattern and were sequentially assigned from the 200 ms NOESY spectrum by way of a "NOESY walk".

Sequential Assignments. The NOESY data were sufficient to observe proton–proton NOEs between the amide proton of one residue and the α-proton of the preceding residue for Cys[2], Ser[3], and Trp[4], Cys[7], Asp[8], and His[9], and Ser[11], Cys[12], and Thr[13].

Resonance assignments for Val[6] and Pro[10] came from their unique spin systems as discussed above. The remaining four residues, Cys[1], Asp[5], Cys[14], and Cys[15], were assigned on the basis of sequential information combined with $H\beta_i$ to HN_{i+1}

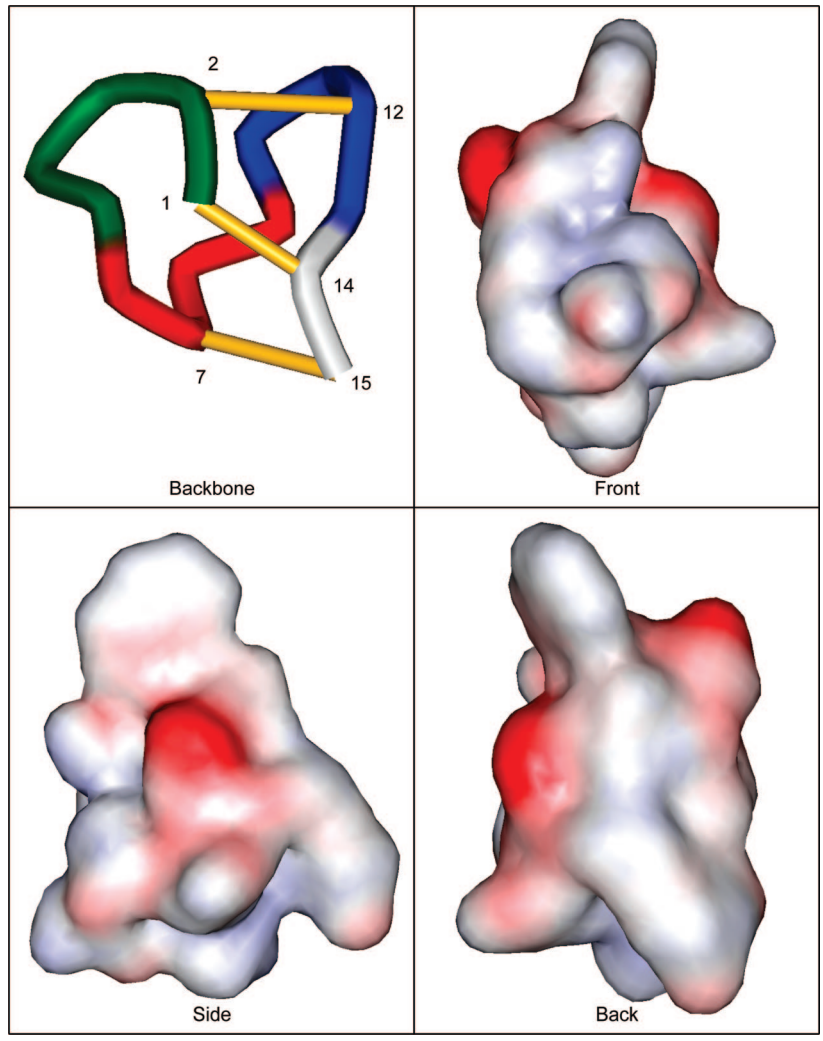

FIGURE 4: Three-dimensional structures of tx3a. Shown is the backbone structure identifying each of the turns (top left), turn 1 from Cys^{1} to Asp^{5} (green), turn 2 between Val^{6} and His^{9} (red), and turn 3 between Pro^{10} and Thr^{13} (blue). The disulfide bonds are colored yellow with the cystine residues numbered. Also shown are the front, side, and back views of the surface of the peptide. Blue regions represent electropositive surfaces, red regions electronegative surfaces, and white and/or faintly colored regions hydrophobic and/or nonpolar surfaces.

cross-peaks from the NOESY spectrum. Off-diagonal resonances were observed for the amide and α-protons of Cys^{2} at 8.04 and 4.14 ppm to the β-protons of Cys^{1} at 2.62 and 2.26 ppm. Likewise, there was a weak NOE interaction between the amide proton of Cys^{1} at 8.09 ppm and the β-protons of Cys^{14} at 2.95 and 2.75 ppm that helped to identify Cys^{14} and verify the assignment of Cys^{1}. The assignment of Cys^{14} permitted the identification and assignment of Cys^{15}. There is an NOE between the amide proton of Cys^{14} at 8.82 ppm and the β-protons of Cys^{15} at 2.14 and 2.01 ppm. Furthermore, there is a cross-peak for the NOE between the amide proton of Cys^{15} and the β-protons of Cys^{7} at 2.89 and 2.08 ppm. The spin system originating at 7.98 ppm was assigned to Asp^{5} by the process of elimination.

DISCUSSION

Proton Assignments. The small size of conotoxin tx3a made it difficult to observe nuclear Overhauser effects in NOESY spectra acquired at 26 °C. A significant improvement was seen at 4 °C, although line widths were significantly broader. The spin systems were easier to resolve at 26 °C due to better spectral resolution, and the NOESY spectra were more informative at 4 °C due to slower molecular tumbling. Thus, spectra acquired at both temperatures were used for assignments.

It was immediately apparent from the spread of amide resonances that conotoxin tx3a adopted a rigid conformation in solution. In general, random coil peptides have amide proton chemical shifts between 8.09 and 8.45 ppm, while those in conotoxin tx3a were between 7.15 and 8.90 ppm (*30*). Similarly, the chemical shifts of α-protons in random coils typically range from 4.4 to 4.8 ppm, while those in conotoxin tx3a resonated between 3.94 and 4.94 ppm. Thus, an ordered secondary structure was expected (*31–35*). The number of constraints per residue and a summary table of all restraints used for structure calculations are provided in Figure 2 and Table 2.

Structure Analysis. The final set of 20 structures for conotoxin tx3a has a mean global backbone rmsd of 0.32 ± 0.07 Å (Figure 3). The backbone of the peptide is well-defined and conserved across all 15 amino acids.

The structure of conotoxin tx3a shows a "triple-turn" motif with turns between residues Cys^{1} and Asp^{5}, Val^{6} and His^{9}, and Pro^{10} and Thr^{13} (Figure 4). The N-terminal turn between

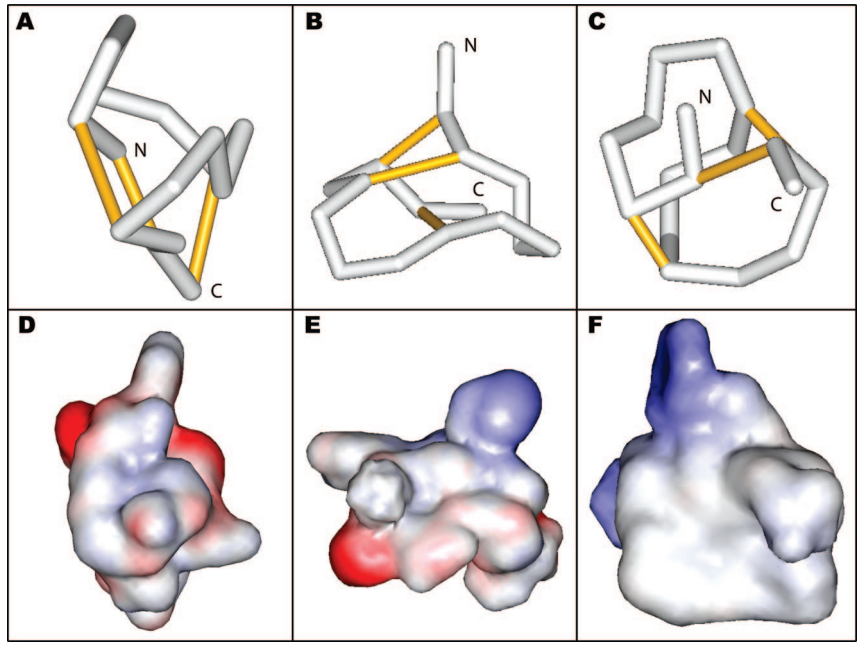

FIGURE 5: Comparison between two m-1 branch peptides, tx3a and mr3e, and one m-2 branch peptide, mr3a. Scaffold structures of tx3a, mr3e, and mr3a are labeled A, B, and C, respectively. Frontal surface structures of tx3a (D), mr3e (E), and mr3a (F), showing the "flying bird" depiction of mr3e and the "plucked chicken" representation for tx3a and mr3a. Blue regions represent electropositive surfaces, red regions electronegative surfaces, and white and/or faintly colored regions hydrophobic and/or nonpolar surfaces.

residues Cys^1 and Asp^5 is a type I β turn held in place by a hydrogen bond between the carbonyl of Ser^3 and the amide proton of Asp^5 (distance of 2.23 Å). In β turn nomenclature (*36*), Cys^2 and Trp^4 represent i and $i + 2$, respectively. Trp^4 has its side chain indole ring pointing away from the core of the structure at the kink of the turn. This distinct protrusion significantly defines the surface of the peptide in this region. A second hydrogen bond between the amide proton of Cys^1 and the carbonyl oxygen of Val^6 further defines the first turn of the molecule. The section of the peptide surrounding Trp^4 and Asp^5 constitutes a hydrophilic patch on surface of the molecule. The side chain carboxylate of Asp^5 and the carbonyl oxygen atoms of Trp^4 and Asp^5 point away from the interior of the peptide. This hydrophilic region is further established by "turn 2."

The second turn occurs between residues Val^6 and His^9. This structural feature is a broad turn constrained by a hydrogen bond between the carbonyl of Cys^7 and the amide proton of His^9 (distance of 2.43 Å) and by the disulfide linkage of Cys^7 and Cys^{15}. The carboxylate of Asp^8 is located at the kink in the turn and points away from the interior of the peptide to present a negatively charged region on the surface of the peptide. It deserves comment that the imidizole ring of His^9 is also oriented away from the interior of the peptide. Thus, there is a region of positive character near the negatively charged Asp^8 carboxylate. The surface created by the second turn of tx3a defines a hydrophilic side of the molecule. Thus, tx3a has a large hydrophilic face on the "front" and "side" regions shown in Figure 4. In contrast, the opposite side of the peptide is largely hydrophobic (see the "back" portion of Figure 4) and corresponds to the location of the methyl and methylene groups of Val^6, Cys^7, Cys^{14}, and Cys^{15}. The only charged group on the surface of the molecule in this region is the C-terminal carboxyl group of Cys^{15}.

The third turn in the peptide is a type III β turn between residues Pro^{10} and Thr^{13}. At the center of this turn is Ser^{11} ($i + 1$). The turn is stabilized by the hydrogen bond between the amide proton of Thr^{13} ($i + 3$) and the carbonyl oxygen of Ser^{11} ($i + 1$) (distance of 1.71 Å). This region of the peptide defining the third turn appears significantly less hydrophilic on the surface than the first or second turn region. Overall, the surface of tx3a is predominantly hydrophilic.

Comparison of m-1 Branch Peptides tx3a to mr3e. Conotoxin tx3a represents the second m-1 branch peptide of the M-superfamily for which a structure is now presented. The structure template for the m-1 branch conotoxins was first described for mr3e (*17*). The triple-turn structure we found for tx3a is substantially different from the "double-turn" motif reported for mr3e despite conserved cystine patterns in the two conotoxins. Differences in the backbone scaffolds of tx3a and mr3e appear to be due to a few key residues. mr3e has two consecutive glycines, Gly^6 and Gly^7, that do not appear in the tx3a sequence. These residues permit the sharp bend in turn 1 of the mr3e structure not seen in tx3a (*37*). Another difference is the number of residues between the cysteine groups. There are 12 residues between C1 and C6 in mr3e and three residues between C3 and C4. In contrast, tx3a has 13 residues between C1 and C6 and four residues between C3 and C4. Maintaining the same disulfide connectivity while changing the spacing of amino acid residues contributes to the observed structural differences between tx3a and mr3e (Figure 5).

tx3a has a more globular shape similar to that of the m-2 branch peptide mr3a, while mr3e has an irregular "flying bird" shape with several amino acid residues jutting out from the peptide backbone (*17*). The topology of tx3a more closely resembles that of mr3a, although the surface of tx3a is considerably more hydrophilic. For example, tx3a contains seven polar and charged residues, while mr3a contains only three (Ser^5, Arg^9, and Hyp^{14}). tx3a has a large hydrophilic region consisting of the carboxylate of Asp^5, the carbonyl oxygen of Cys^7, the carboxylate of Asp^8, and the imidizole ring of His^9 located primarily on the front face of the

molecule. In spite of these differences, the two peptides exhibit similar excitatory physiological effects in mice and not toward fish. Thus, the triple-turn motif appears to be important for the excitatory behavior seen in mice.

It is well established that m-1, m-2, and m-3 peptides elicit a different symptomatology when injected into mice and fish than do their larger m-4 counterparts. The m-4 branch peptides, consisting of the μ-, ψ-, and κM-toxins, are found primarily in fish-hunting *Conus* species. It is not surprising that the fish hunters require biological warfare agents that rapidly immobilize their fast-moving prey. The m-4 peptides are generally paralytic in nature. In contrast, the m-1, m-2, and m-3 peptides are primarily found in the venoms of mollusk and worm-hunting cone snails. The physiological response that these smaller peptides elicit is excitatory. When injected with tx3a, mice become hyperactive with small doses and have seizures resulting in death with larger doses. mr3a is known to cause barrel rolling seizures in mice. There are no reports of activity by m-1, m-2, or m-3 conotoxins in fish. Although experiments have not been conducted with snails or worms, it is possible that exciting a snail or worm prey is advantageous by driving the "feast" from its protective habitat. Although the receptors for these peptides are not known, it is clear that they are active in a distinctive manner from their m-4 counterparts and the topology generated by the triple-turn motif seen in tx3a and mr3a is important for their observed activities. The role of the triple-turn scaffold in the interaction among tx3a, mr3a, and their target receptors will not be completely understood until their receptors are identified.

ACKNOWLEDGMENT

We thank Professor Baldomero M. Olivera, Dr. J. Michael McIntosh, Richard Jacobsen, and Mikal-Anne Waters for assistance and advice on this project and Sean Ruettgers for technical support.

REFERENCES

1. Kohn, A. J., Saunders, P. R., and Wiener, S. (1960) Preliminary studies on the venom of the marine snail Conus. *Ann. N.Y. Acad. Sci. 90*, 706–725.
2. Myers, R. A., Cruz, L. J., Riviera, J. E., and Olivera, B. M. (1993) Conus peptides as chemical probes for receptors and ion channels. *Chem. Rev. 93*, 1923–1936.
3. Olivera, B. M., Rivier, J., Clark, C., Ramilo, C. A., Corpuz, G. P., Abogadie, F. C., Mena, E. E., Woodward, S. R., Hillyard, D. R., and Cruz, L. J. (1990) Diversity of Conus neuropeptides. *Science 249*, 257–263.
4. Olivera, B. M., Gray, W. R., Zeikus, R., McIntosh, J. M., Varga, J., Rivier, J., de Santos, V., and Cruz, L. J. (1985) Peptide neurotoxins from fish-hunting cone snails. *Science 230*, 1338–1343.
5. Hann, R. M., Pagán, O., and Eterovic, V. A. (1994) The 101-conotoxins GI and MI distinguish between the nicotinic acetylcholine receptor agonist sites while SI does not. *Biochemistry 33*, 14058–14063.
6. RCSB Protein Data Base. http://www.rcsb.org/pdb/advSearch.do. Search Term: conotoxin (accessed November 2, 2007).
7. Chi, S., Kim, D., Olivera, B. M., McIntosh, J. M., and Han, K. (2004) Solution conformation of α-conotoxin GIC, a novel potent antagonist of α3β2 nicotinic acetylcholine receptors. *Biochem. J. 380*, 347–352.
8. Everhart, D., Cartier, G. E., Malhotra, A., Gomes, A. V., McIntosh, J. M., and Luetje, C. W. (2004) Determinants of potency on α-conotoxin MII, a peptide antagonist of neuronal nicotinic receptors. *Biochemistry 43*, 2732–2737.
9. McIntosh, J. M., Azam, L., Staheli, S., Dowell, C., Lindstrom, J. M., Kuryatov, A., Garrett, J. E., Marks, M. J., and Whiteaker, P. (2004) Analogs of α-conotoxin MII are selective for α6-containing nicotinic acetylcholine receptors. *Mol. Pharmacol. 65*, 944–952.
10. Loughnan, M. L., and Alewood, P. F. (2004) Physico-chemical characterization and synthesis of neuronally active α-conotoxins. *Eur. J. Biochem. 271*, 2294–2304.
11. Nicke, A., Wonnacott, S., and Lewis, R. J. (2004) α-Conotoxins as tools for the elucidation of structure and function of neuronal nicotinic acetylcholine receptor subtypes. *Eur. J. Biochem. 271*, 2305–2319.
12. Millard, E. L., Daly, N. L., and Craik, D. J. (2004) Structure-activity relationship of α-conotoxins targeting neuronal nicotinic acetylcholine receptors. *Eur. J. Biochem. 271*, 2320–2326.
13. Al-Sabi, A., Lennartz, D., Ferber, M., Gulyas, J., Rivier, J. E., Olivera, B. M., Carlomagno, T., and Terlau, H. (2004) κM-Conotoxin RIIIK, structure and function novelty in a K^+ channel antagonist. *Biochemistry 43*, 8625–8635.
14. Bordia, T., Grady, S. R., McIntosh, J. M., and Quik, M. (2007) Nigrostriatal damage preferentially decreases a subpopulation of α6β2 nAChRs in mouse, monkey, and Parkinson's disease striatum. *Mol. Pharmacol. 72*, 52–61.
15. Corpuz, G. P., Jacobsen, R. B., Jimenez, E. C., Watkins, M., Walker, C., Colledge, C., Garrett, J. E., McDougal, O., Li, W., Gray, W. R., Hillyard, D. R., Rivier, J., McIntosh, J. M., Cruz, L. J., and Olivera, B. M. (2005) Definition of the M-conotoxin superfamily: Characterization of novel peptides from molluscivorous Conus venoms. *Biochemistry 44*, 8176–8186.
16. Han, Y., Wang, Q., Jiang, H., Liu, L., Xiao, C., Yuan, D., Shao, X., Dai, Q., Cheng, J., and Chi, C. (2006) Characterization of novel M-superfamily conotoxins with new disulfide linkage. *FEBS J. 273*, 4972–4982.
17. Du, W., Han, Y., Huang, F., Li, J., Chi, C., and Fang, W. (2007) Solution structure of an m-1 conotoxin with a novel disulfide linkage. *FEBS J. 274*, 2596–2602.
18. McDougal, O. M., and Poulter, C. D. (2004) Three-dimensional structure of the mini-M conotoxin mr3a. *Biochemistry 43*, 425–429.
19. Ott, K., Becker, S., Gordon, R. D., and Rüterjans, H. (1991) Solution structure of μ-conotoxin GIIIA analyzed by 2D-NMR and distance geometry calculations. *FEBS Lett. 278*, 160–166.
20. Hill, J. M., Alewood, P. F., and Craik, D. J. (1996) Three-dimensional solution structure of μ-conotoxin GIIIB, a specific blocker of skeletal muscle sodium channels. *Biochemistry 35*, 8824–8835.
21. Van Wagoner, R. M., and Ireland, C. M. (2003) An improved solution structure for ψ-conotoxin PIIIE. *Biochemistry 42*, 6347–6352.
22. Van Wagoner, R. M., Jacobsen, R. B., Olivera, B. M., and Ireland, C. M. (2003) Characterization and three-dimensional structure determination of ψ-conotoxin PIIIF, a novel noncompetitive antagonist of nicotinic acetylcholine receptors. *Biochemistry 42*, 6353–6362.
23. Wüthrich, K. (1986) *NMR of Proteins and Nucleic Acids*, Wiley, New York.
24. Bax, A. (1989) Two-dimensional NMR and protein structure. *Annu. Rev. Biochem. 58*, 223–256.
25. Rance, M., Sørensen, O. W., Bodenhausen, G., Wagner, G., Ernst, R. R., and Wüthrich, K. (1983) Improved spectral resolution in COSY proton NMR spectra of proteins via double quantum filtering. *Biochem. Biophys. Res. Commun. 117*, 479–485.
26. Jeener, J., Meier, B. H., Bachmann, P., and Ernst, R. R. (1979) Investigation of exchange processes by two-dimensional NMR spectroscopy. *J. Chem. Phys. 71*, 4546–4553.
27. Braunschweiler, L., and Ernst, R. R. (1983) Coherence transfer by isotropic mixing: Application to proton correlation spectroscopy. *J. Magn. Reson. 53*, 521–528.
28. Keepers, J. W., and James, T. L. (1984) A theoretical study of distance determinations for NMR. Two-dimensional nuclear Overhauser effect spectra. *J. Magn. Reson. 57*, 404–426.
29. Güntert, P., Mumenthaler, C., and Wüthrich, K. (1997) Torsion angle dynamics for NMR structure calculation with the new program DYANA. *J. Mol. Biol. 273*, 283–298.
30. Bundi, A., and Wüthrich, K. (1979) Proton NMR parameters of the common amino acid residues measured in aqueous solutions of the linear tetrapeptides H-Gly-Gly-X-L-Ala-OH. *Biopolymers 18*, 285–297.
31. Wishart, D. S., Sykes, B. D., and Richards, F. M. (1991) Relationship between nuclear magnetic resonance chemical shift and protein secondary structure. *J. Mol. Biol. 222*, 311–333.

32. Wishart, D. S., Sykes, B. D., and Richards, F. M. (1991) Simple techniques for the quantification of protein secondary structure by proton NMR spectroscopy. *FEBS Lett. 293*, 72–80.
33. Wishart, D. S., Sykes, B. D., and Richards, F. M. (1992) The chemical shift index: A fast and simple method for the assignment of protein secondary structure through NMR spectroscopy. *Biochemistry 31*, 1647–1651.
34. Wishart, D. S., Bigam, C. G., Holm, A., Hodges, R. S., and Sykes, B. D. (1995) ^{1}H, ^{13}C, and ^{15}N random coil NMR chemical shifts of the common amino acids. I. Investigations of nearest-neighbor effects. *J. Biomol. NMR 5*, 67–81.
35. Volkman, B. F., Nohaile, M. J., Amy, N. K., Kustu, S., and Wemmer, D. E. (1995) Three-dimensional solution structure of the N-terminal receiver domain of NTRC. *Biochemistry 34*, 1413–1424.
36. Rose, G. D., Gierasch, L. M., and Smith, J. A. (1985) Turns in peptides and proteins. *Adv. Protein Chem. 37*, 1–109.
37. Voet, D., and Voet, J. G. (2004) *Biochemistry*, pp 222–223, John Wiley & Sons, Inc., New York.

BI702388B